Scale-up of Flotation Processes

Mikhail Burstein and Lev Filippov

January 2010

Publication Number: CSRCR2010-01

Computational Science & Engineering Faculty and Students Research Articles

Database Powered by the Computational Science Research Center Computing Group

COMPUTATIONAL SCIENCE & ENGINEERING

SAN DIEGO STATE UNIVERSITY

Computational Science Research Center
College of Sciences
5500 Campanile Drive
San Diego, CA 92182-1245
(619) 594-3430

Scale-up of Flotation Processes

Dr. Mikhail BURSTEIN, Computational Science Research Center, San Diego State University, San Diego, CA, USA, Burstein@mail.sdsu.edu
Professor Lev FILIPPOV, Laboratoire Environnement et Minéralurgie, LEM UMR 7569 CNRS, Nancy, France, Lev.Filippov@ensg.inpl-nancy.fr

1 Introduction

Flotation is the core separation stage in mineral processing for base metal ores; it is also widely used in coal fines preparation, waste water treatment, and other applications where the difference in the bubble-particle (or bubble-droplet) attachment ability (i.e. hydrophobic properties) can be the basis for separation. In the vast majority of applications, the three phases are present in the machine: liquid carrier (typically, water-based), phase to be separated or removed (solid particles or insoluble liquid droplets), and the gas phase onto which the attachment occurs (most commonly, air).

Due to the wide range of systems utilizing flotation separation, the equipment used for the process varies. It can be classified based on the method to generate and to introduce the gas bubbles (dissolved-air, forced injection, suction), the level of turbulence (impeller or impellerless), relative direction of phase movement (reactor-separator, bank of several cells, countercurrent column). Capacities of the machines can be as little as a portion of a cubic centimeter or as large as several hundreds of cubic meters.

All of the above makes creating the techniques for flotation scale-up particularly challenging.

In addition to that, unlike many other separation processes, increased duration of the flotation separation does not necessarily improve its metallurgical results. While this is generally true for waste water treatment, raising the time of bubble/particle exposure in mineral flotation typically increases the recovery of component to be collected with the froth, but leads to product grade deterioration. Therefore, determining the correct arrangement and size of the flotation cells based on batch and pilot test results (scaling-up) is extremely important for the overall results.

Scale-up should also include a methodology to optimize the flowsheet which (in case of mineral flotation) typically includes rougher, scavenger and cleaner stages with recycling of intermediate products into the previous stage (optionally including additional reagent treatment and/or regrinding).

Despite all considerations, the typical approach is to determine the “right” parameters in lab-scale tests (including conditioning and separation time, etc.) and then to apply them to the industrial-scale operation using an empirical “scale-up factor”.

Based on the complexity and multifaceted nature of the problem, hierarchical model is required to analyze all the aspects and to propose a reliable scale-up approach.

This paper summarizes the major works done by the type of flotation machinery used.

2 Flotation scale-up fundamentals

The simplest approach is to consider flotation as the process following the first-rate kinetics. Assuming that particles do not interact with each other and do not "compete" for the space on bubble surface (in slurry and in froth), this approach is adequate under steady-state conditions (i.e., the stable froth has been formed and is discharging, gas holdup and velocity distribution reached the final pattern, etc.).

Rate of the first-order kinetics equation (often referred to as flotation rate K, min^{-1}) represents a probability of a particle (more precisely, a unit mass of the component in question) transfer into concentrate per unit time. Change of the constant depending of the scale of the flotation machine is the factor determining the scale-up considerations.

It should be noted that (unlike reaction rates in chemical engineering) flotation rate depends upon particle composition and size as well as upon its surface properties, reagent adsorption and other factors. Therefore, each component may be represented by its continuous flotation rate distribution F(K). Formally speaking, deformation of this set of distributions at scale-up is determining results of industrial-scale process based on given pilot/batch results. Given the identical chemical environments, this deformation can be attributed to the differences in aeration and hydrodynamics between machines of different scale. Analysis of the differences should be based on studying the physics of the flotation process.

In addition to that, at continuous flotation, particle retention time is not constant (unlike at batch flotation experiments); hence, dispersion of the residence time distribution (RTD) E(t) should be taken into consideration as the factor reducing metallurgical performance (both recovery and grade) comparing to those in batch tests under the identical otherwise conditions and flotation time.

Overall, recovery R of a component in continuous flotation can be calculated as [1, 2]

$$R = \iint F(K)E(t)(1-\exp(-Kt)dKdt \qquad (1)$$

If flotation rate distribution had a rectangular shape, batch flotation kinetics would follow Klimpel equation

$$R(t) = 1- (1-\exp(-K_{max}t)/K_{max}t) \qquad (2)$$

(K_{max} is the highest flotation rate of the given component under the given conditions). While simple to interpret, this equation represents another extreme case opposite to an assumption that all particles containing given component have equal floatability. In reality, the flotation rate distribution has a bell shape, similar to the gamma-distribution. In addition to that, certain part of material (or its component) would not float even at infinite separation time and is represented by the fraction of K=0.

In addition to bubble/particle attachment/detachment dynamics determining selectivity of the separation, flotation comprises of several other distinct "subprocesses" including particle collision with the bubble, transport of loaded bubbles into froth, particle entrainment (upward movement of fine unattached particles into froth), froth transport, syneresis, etc. Most of these processes are not

dependent on particle surface properties ("floatability"). Particle flocculation and reagent adsorption also occur in flotation cells. To have adequate understanding of flotation scale-up, all of these processes should be prioritized and analyzed.

For capture to occur between a bubble and a hydrophobic particle, they must first undergo a sufficiently close encounter, a process that is controlled by the hydrodynamics governing their approach in the aqueous environment in which they are normally immersed [3]. Should they approach quite closely, within the range of attraction surface forces, the intervening liquid film between the bubble and particle will drain, leading to a critical thickness at which rupture occurs. Movement of the three-phase contact line (the boundary between the solid particle surface, receding liquid phase, and advancing gas phase) then occurs, until a stable wetting perimeter is established. This sequence of drainage, rupture, and contact line movement constitutes the attachment process. A stable particle–bubble aggregate is thus formed.

The particle may only be dislodged from this state if it is supplied with sufficient ~~kinetic~~ energy to equal or exceed the attachment energy; thus a process of detachment can occur.

The collection (or capture) efficiency E_{coll} of a bubble and a particle is often defined as

$$E_{coll} = E_c E_a E_s$$

where E_c is the collision efficiency, E_a is the attachment efficiency, and E_s is the stability efficiency of the bubble–particle aggregate. This dissection of capture efficiency into three processes, proposed many years ago, focuses attention on the three regions of bubble–particle capture around the bubbles where, in order, hydrodynamic interactions, surface forces, and forces controlling bubble–particle aggregate stability are dominant [4, 5]. Each component in the equation above depends upon particle size and other characteristics as well as upon local hydrodynamics in the flotation cell.

It should be noted that this approach ignores two important factors: (1) flotation is a kinetic process and most of "efficiencies" should be considered as "rates" or "intensities"; (2) all of the processes are reversible, i.e. particle can repeatedly undego attachment/detachment stages in slurry and in froth (most profound for coarse particles and for impeller machines with intensive mixing and columns with deep washed froth layer and cleaning zone) before it eventually is removed into the concentrate launder. Based on that, the structure of subprocesses can be considered as Markov chain and the overall rate can be calculated accordingly [6].

An attempt to link overall kinetics with subprocess structure including entrainment and froth characteristics and to the physical parameters is presented by Ralston and co-authors [7].

When flotation state is considered as local dynamic equilibrium between attachment and detachment processes, it becomes the standard Computational Fluid Dynamics (CFD) task [8], which can be described (including the limit of particle load on bubble of certain size β) for a given finite element as

$$dN_{p1}/dt = -k_1 N_{p1} N_b (1 - \beta) + k_2 N_a \qquad (3)$$

Combining this source/sink balance equation with multi-phase flow equations for the conservation of mass, momentum and turbulence quantities and description of bubble size distribution allows representation of transport processes of free and attached particles in the volume of the cell. Having dependencies of attachment and detachment rates upon physical parameters and those from the cell size and geometry as well as from operating parameters (impeller tip speed, air and feed flow rates, e.a.), one can build the scale-up simulation from the first principles [9].

Particle retention time in froth t_f also affects kinetics, and, therefore, the metallurgical results as particles can drop from the froth due to drainage in Plateau canals as well as due to syneresis. According to [10], K decreases exponentially with t_f and raises linearly with bubble surface area flux but the relationship is dependent on the cell size and, therefore, not directly useful for scale-up. When t_f is divided by a typical cell dimension to take into account the effect of froth transportation distance in cells of different sizes, the relationship between K and the "specific froth residence time" fits the data better and is found to be independent of cell size.

3 Scale-up in impeller cells

During the last 100 years, this type of machines has been the main equipment for the flotation of ores and coal. They are manufactured by several leading vendors which are developing their own phenomenological recommendations for selecting the type and sizes of cells for a given task.

The cell in these machines can be divided into two distinct zones: within the impeller (mechanism) and outside it. There is no single opinion whether “stable” flotation attachment occurs inside the impeller. While the probability of collision in this zone with intensive turbulent mixing is high, the contact time between particle and bubble is very short. The relationship between the contact time and “induction time” necessary to form the “three-phase wetting perimeter” determines the probability of particle attachment to a bubble following their collision.

Also, flotation attachment is reversible for relatively coarse particles. The gradient of liquid velocity in the vicinity of the bubble surface determines the magnitude of shear forces. Balance of these forces, gravity, particle inertia, and attachment forces between particle and bubble results in stability of the flotation aggregates.

Based on that, mechanism of the flotation attachment may differ in the impeller zone and outside it, as well as for fine and for coarse particles of different specific gravity.

Obviously, the differences in impeller geometry, size and its tip speed between laboratory, pilot and industrial cells are the major reason for discrepancies in metallurgical results at identical nominal retention time.

The fundamental research of particle-bubble collision in highly-turbulent flows is done by H. Schubert [11]. One should note that the induction time is also dependent on the pressing force between particle and bubble and is shorter when particle approach to the bubble is at high velocities rather than that at quiescent sliding.

Intensity of collisions and contact time and its dependence on particle and bubble sizes as well as local air holdup and turbulence parameters are used by Koh et al as the input parameters for CFD modeling [6]. They found that the limiting factor is often not the collision or attachment rate, but insufficiency of the bubble surface area for attachment of all material to be recovered into froth. This is even more important for the flotation of ultrafine particles having high specific surface area when bubble

carrying capacity is lower (the mass of particles which can be attached to and carried by the unit bubble surface is smaller).

Experimental analysis of the influence of energy dissipation and superficial air velocity in the cell on undistributed flotation rate constant for a given size fraction is given by Newell and Grano [12]. It has been found that, in the aeration range studied, flotation rate K grows linearly with the bubble area flux. N^3D combination defining energy dissipation (N is rotational speed of the impeller and D is its diameter) has been found to be a good scale-up criterion. It should be noted, though, that no research has been conducted using cells with capacity over 50 dm^3 in this work.

In addition to lower flotation rates in large-scale flotation cells, the dispersion of Residence Time Distribution [RTD, E(t)] there is typically higher. While in batch flotation tests, all particles have equal flotation time, it is not the case in a continuous process. Some particles can shortcut to the tailings discharge while others circulate in the bank of cells significantly longer than the nominal retention time calculated as the ratio of the volumetric slurry flowrate to the volume of slurry in the bank. Assuming high-intensity mixing in a flotation cell and low return flow between the cells (which is a good approximation for flotation cells with the baffles between them), the RTD follows the "cell model" which has been extensively studied in chemical engineering.

For N continuous perfect mixers-in-series, with a total residence time τ, the following equation has shown a good agreement to represent the residence time distribution of the rougher plant [13]

$$E(t) = t^{N-1}e^{-(Nt/\tau)}/((\tau/N)^N\Gamma(N)) \qquad (4)$$

This expression can be substituted in equation (1) where $F(K)$ is the flotation rate distribution in the industrial-scale machine.

If (though no physical grounds for the assumption can be given) flotation rate distribution is uniform from K = 0 to $K = K_{max}$ (see eq.(2) above) and that the recovery after infinite flotation time is R_{max}, Yianatios, *et al.* [13] found that following simple relationships allow adequate prediction of plant results from batch tests:

$$t/T = k_{max}/K_{max} \qquad (5)$$
$$r(t)/R(T) = r_{max}/R_{max} \qquad (6)$$

where t, T – flotation time in lab and industrial cell at the point of optimum separation at identical flotation regime, r, R – recoveries at that time in these cells, r_{max}, R_{max} – recoveries in infinite time in both cells [1].

Recovery into froth by the true flotation in the commercial flotation apparatus can be predicted based on laboratory test results using the technique which includes the following:
1. Conduct a kinetic test in a laboratory apparatus.
2. Evaluate particle size distribution in the feed $f(d_p)$ and in the products of the kinetic test.
3. Evaluate the dependences of recovery and yield in batch processes upon the time for each size fraction $(R_{ld}(t))$ and $Y_{ld}(t)$).
4. Using the chosen formula of the function, assess $K_l(d_p)$ for laboratory and $K_c(d_p)$ for commercial apparatus. It requires estimation of the aeration characteristics of laboratory and commercial apparatus and calculation of average relative velocities of

particles and bubbles.
5. Solve the following equation for $f_d(P_a)$

$$1 — R_{ld}(t) = \int f_d(Pa) exp(— K_c(d_p) P_a t) dP_a$$

i.e. assess the "physico-chemical floatability" distribution of components in each size fraction.
6. Evaluate the density of residence time distribution for material of d_p size in an apparatus of continuous operation $E_d(t)$.
7. Substitute the obtained relationships into the formula

$$R_c = \iiint f(d_p)\, f_d(P_a)\, [1 — exp(— K_c(d_p) P_a t]\, E_d(t) dP_a d(d_p) dt$$

and calculate the expected values of recovery and yield under commercial conditions.

The same recovery R in a commercial apparatus can be achieved at different values of the volumetric slurry flow rate ~~determining the required height of the collection zone~~. The material can be either processed in several apparatuses operated in parallel or in the same number of cells in series. In absence of mutual influence of particles, sufficient air flow rate and insignificant back mixing in a bank of flotation cells, the same process results will be observed in the apparatuses operated in parallel and in series since average retention time is the same. It is difficult to make a comprehensive analytical evaluation of the mutual influence of the particles. It is connected with the processes of aggregate formation, hindered bubble/particle attachment, re-attachment in froth, changes in the liquid phase composition during flotation, and product grade reduction resulting from back mixing. Therefore, final recommendations on optimum design of a flotation circuit should be based on the analysis of experimental results. An increase of feed flow rate Q_l at a consistent solids feed flow rate (reduction of slurry density) down to certain limits is of little importance for the microstructure of flow patterns, hence, for flotation subprocesses. Since the separation curve $S(K,t)$ and the RTD profile change insignificantly, an increase of Q_l can be made up for by increasing flotation time without changes in recovery and concentrate grade. Commonly, slurry velocity variations are small compared to the intensity of turbulent pulsations; hence, the local flow parameters are practically unaffected.

According to some studies, non-selective entrainment of fines into froth in the wake of bubbles or by upward local flows in highly-mixed impeller cell cannot be neglected. Share of true flotation vs. entrainment is determined in [14] .The entrainment of the fine particles can be directly related to the water recovery and can be estimated by mineral recovery in the absence of collector (providing natural floatability is small).

4 Scaling-up methods for flotation columns

4.1 General approach

4.1.1 Principle of column operation

Extensive use of flotation columns necessitated development of a simple and accurate method to calculate their design and process parameters based on pilot test

results [15, 16]. Column flotation basics and major factors should be determined to develop scale-up approach.

Flotation column is a vertical chamber of round or rectangular cross-section. Its height-to-diameter ratio should exceed 5:1. It includes the following units (Figure 1): column body, sparger, feed distributor, and froth launder.

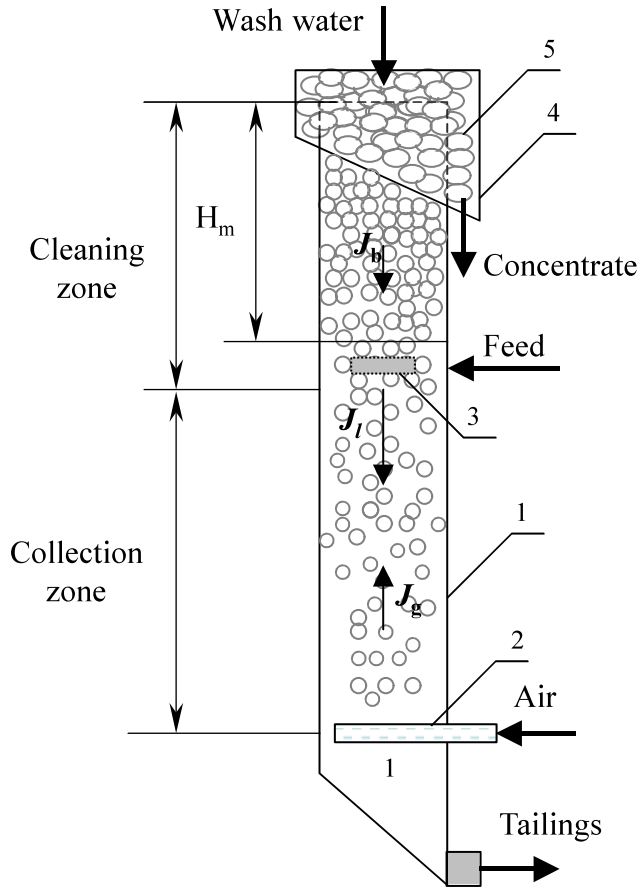

Figure 1 Diagram of column flotation: 1-column body, 2-sparger, 3-feed distributor, 4- froth launder, 5-froth.
H_m: froth depth; J_b: superficial bias velocity of the wash water; J_l: superficial feed velocity; J_g : superficial gas velocity.

A column is comprised of two sections:

- Collection zone between the sparger and feeder level. According to Sastry [17], Yianatos [19], and Finch and Dobby[18], this zone should have the height of 75-80% of the overall column.
- Cleaning zone which is effective only if wash water is added at the froth top. This zone is the same as froth if the column is fed at the froth/slurry interface level. If feed enters below the froth/slurry interface, then the cleaning zone includes a part of the column. This zone is needed for froth drainage to avoid hydrophilic particles entrainment into the concentrate.

Feed slurry after reagent conditioning enters the column generally at the froth/slurry interface or below. This area serves for the contact of froth, slurry, wash water and rising bubbles. Bubbles are generated at the sparger (2) located near the

column (1) bottom. Loaded bubbles are accumulated above the slurry forming froth (5) which overflows to the launder.

Column diameter (d_C) determines the machine capacity and flotation efficiency. Diameter increase leads to a rise in the dispersion number D ($D \cong d_C^{1/3}$). This causes change of metallurgical results at scale up from lab or pilot columns to industrial units [20].

Columns of large diameter can have slurry circulation of larger scales caused by the following :

- particle settling at the wall part of the column due to lower aeration of the slurry there;
- high air holdup in the axial portion causes upward slurry movement and fine particle entrainment;
- profile of liquid velocities caused by slower flow near the walls.

Column height H_C and height-to-diameter ratio (H_C/d_C) are the major parameters which determine industrial column design and performance. Increased H_C/d_C ratio leads to lower upward slurry flows, thus, it increases recovery and selectivity. Typically, columns of over 10 m high are used in the industry.

At early ages of flotation columns at plant operation, it has been commonly assumed that the higher is the column, the better performance it allows to obtain. Increased column height can really improve bubble surface utilization and their mineral load. But it also can cause the following negative phenomena:

- bubble surface is insufficient for the mineral to be recovered,
- bubble rise velocity decreases with the load and, ultimately, some mineral/bubble aggregates may have zero buoyancy,
- overly mineralized froth requires increased wash water dosage which can cause particle drop from the froth.

Superficial feed velocity J_l is the ratio of the volumetric feed flow rate Q_f to the column cross-section A_C. It is expressed in cm/s:

$$J_l = \frac{Q_f}{A_c} = \frac{4Q_f}{\pi d_c^2}$$

Superficial feed velocity determines the column flotation results.
It defines the value of the following parameters:

1) slurry residence time,
2) liquid velocity J_l,
3) bubble rise velocity.

Due to the countercurrent nature of the flows, air bubbles (or particle/bubble aggregates) should exceed certain velocity to reach the froth, otherwise, they will report to tailings. This limits utilisation of fine bubbles.

Slurry aeration is normally described by ***air holdup*** ε_g. It can be measured by hydrostatic pressure profiling along the column height due to the presence of the gas phase (bubbles) in the slurry. Gas holdup depends on air flowrate and column capacity. Gas phase is measured by the superficial gas (air) velocity J_g (cm/s).

$$J_g = \frac{Q_g}{A_c} = \frac{4Q_g}{\pi d_c^2}$$

where Q_g is the gas flow.

Flotation column always has optimal J_l/J_g ratio. Effect of air flowrate on flotation performance at a constant feed flow has a complex nature. Increased superficial air

velocity causes raise in the gas holdup and in the average bubble size. Bubble surface area defines bubble carrying capacity while increased bubble diameter reduces the collision probability. Increased aeration also causes bubble coalescence. Overall result of the above processes lead to the maximum point on the recovery curve as a function of superficial gas velocity (Figure 2).

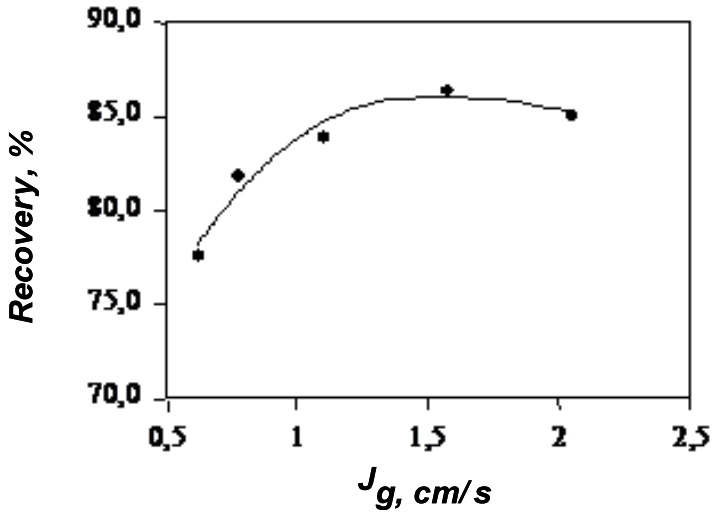

Figure 2. Effect of superficial air velocity upon recovery in the collection zone for 3.8m dia. column (adapted from [21]).

Sharp increase in air flow can cause formation of large bubbles due to coalescence, intensive slurry mixing and bursting and, as a result, steep deterioration of flotation process. Reduced superficial gas flowrate at constant gas holdup can cause lower recovery despite of increased particle/bubble collision efficiency. This is explained by high mineral load on fine bubbles and their sinking.

Bubble diameter depends on sparger type and column feed composition and properties. Bubble average diameter and size distribution are key factors of successful column operataion. Photogrpahic measurement and modeling of bubble sizes can be conducted for liquid/gas systems, but not for three-phase flotation slurries. It can be estimated in Flotation Columns from Drift Flux Analyses [22]. For two-phase sustems, one can assume that for identical spargers, initial bubble size distribution is the same for pilot- and industrial-scale columns.

Retention time. All factors described above affect particle residence time t_p, which determines recovery in the collection zone. Slurry retention time can be calculated based on volumetric tailing flow Q_r and collection zone volume [18, 19, 23]:

$$\tau_l = \frac{A_c H_c (1 - \varepsilon_g)}{Q_r}$$

Particle residence time τ_p is higher for smaller particles [20]. For countercurrent flow, the following expression can be derived:

$$\tau_p = \tau_l \frac{J_l/(1-\varepsilon_g)}{J_l/(1-\varepsilon_g)+U_{sp}}$$

where U_{sp} is the particle settling velocity in slurry calculated from Maslyah [24] equation, and J_l is the superficial slurry velocity. The difference of slurry retention time and particle residence time is more profound for coarse particles. According to the experimental results Dobby and Finch at superficial slurry flowrate of 1-2 cm/s, the retention time for particles of 120 μ m size is just 60% of that of slurry [20]. For fine light particles, retention time is close to the one of the liquid.

For industrial-scale columns, particles of -100 μm fraction are distributed identical to the liquid phase. This means that flotation column turbulence allows to ignore effect of difference in sizes for such particles. These vortices influence slurry and particle residence time distribution as well as air and wash water flowrates.

4.1.2 Approach to scaling

A considerable number of models have been proposed for description of different aspects of column flotation. But any one of them taken separately does not allow calculation of the parameters of the apparatus. An algorithm comprising a number of stages is required to solve this problem. The technique proposed by Canadian researchers [15, 18] is the most widely used. It includes the following stages:

1. Evaluation of flotation rate constant of each component by laboratory test results;
2. Calculation of recovery in the collection zone;
3. Calculation of overall recovery in the column;
4. Assessment of the degree of bubble loading.

Let us consider each of the stages of column scale-up. A curve similar to that of flotation kinetics for a batch apparatus can be obtained in a laboratory column of low height (1-2 m). The tests are run with several cleaner stages for tailings reprocessing and analysis of all the concentrates. Under conditions close to plug flow in a laboratory column i.e. there is no turbulent diffusion (this is true for columns of very small diameter), the obtained results make up a flotation kinetics curve from which the required rate constant can he determined. Since material floatability differs considerably, Dobby and Finch proposed to distinguish fractions of high and low flotation rates in each component of the floated material [15]. Flotation rate constant and the proportion of each fraction are evaluated from the kinetics curve. If the diffusional flow in a laboratory column cannot he neglected, the value of K is calculated by the iterative solution of an equation similar to equation proposed by Levenspiel [25] including the sum of recovery values of the two fractions. The air flow required for maximum recovery is considered to be optimum and is evaluated experimentally. It is difficult to predict the effect of aeration upon process results since it influences both bubble size and capture efficiency. Thus, the type of the sparger in a laboratory and commercial column should be the same to provide the same bubble size distribution. Calculation of the optimum height of the collection zone from a derivative of Levenspiel equation is the second stage of scaling-up.

4.2 SIMULATION OF FLOTATION COLUMNS

Scale up techniques is based on certain models of process and machine. Among many approaches to flotation theory, mass transfer equations are the most used [2, 16, 18, 26, 27, 28, 29]. Most of publications refer to classical reactor design approach which allows estimating industrial apparatuses parameters if process kinetics and hydrodynamics are known:

$$\frac{dC}{dt} = - KC + \text{div}\,(U\,C) + \text{div}\,(D\ \text{grad}\ C)$$

where *K* is flotation kinetic rate, *D* is the dispersion coefficient.

4.2.1 Collection zone recovery

Axial dispersion model is largely used for flotation in columns. This theory is based on the assumption that the fluid transfer in cylindrical cell is determined by the phase relative velocities and the dispersion coefficient. Radial flow loops are considered insignificant. The column is assumed to behave as a non-ideal plug flow reactor.

Under this approach, equation for particle concentration *C* in the collection zone can be presented as

$$D\frac{d^2C}{dx^2} - U_i\frac{dC}{dx} - \frac{dC}{dt} = 0\ ,$$ where *x* is the axial coordinate.

Analytical solution of the equation by Levenspiel (1972) defines mineral recovery in the collection zone for the first-order kinetics:

$$R = 1 - \frac{4a\exp(1/2N_d)}{(1+a)^2\exp(a/2N_d) - (1-a)^2\exp(-a/2N_d)}$$

where $a = (1+K\tau N_d)^{1/2}$
N_d= vessel dispersion number
L = collection zone height
d_c= column diameter
τ= mean residence time

If the intensity of the elementary flotation process is considerably higher than the particle detachment and entrainment rates, equation (1), having an analytical solution (2), can be used to describe the steady state conditions for particles with K value of the kinetic constant. Under the assumptions made, the right part of the equation presents the separation characteristic of column flotation. It shows the dependence of material distribution between the products of the operation upon the separation criterion K.

For practical use of equation (2) Levenspiel's diagram has been modified (Figure 3). The diagram was complemented by the isolines of equal values of the modified Peclet number

$Pe^* = (U_p + U_l)H/D$

where H is the height of plug flow apparatus providing recovery equal to that in a column of H height with dispersion coefficient D.

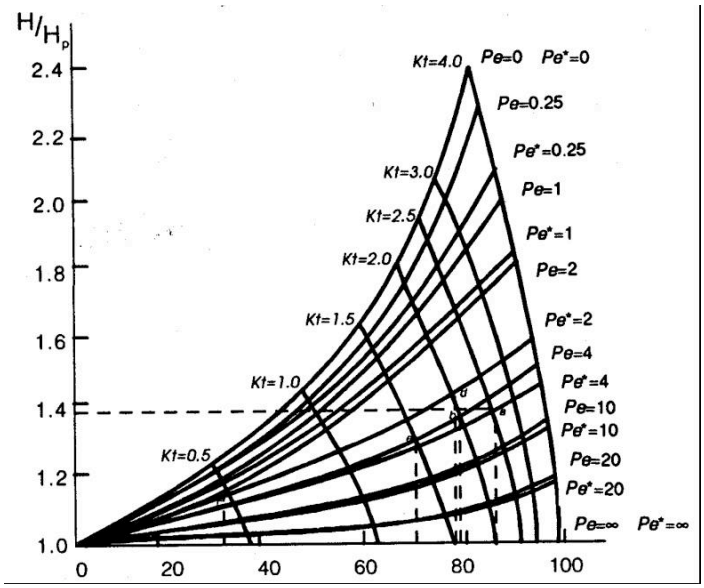

Figure 3. Modified diagram for evaluation of collection zone height based on axial dispersion equation (mass transfer model) and first-order kinetics (flotation model).

The modified diagram allows the evaluation of the required height H from the calculated H_l value. The practical use is as follows: Material recovery to tailings is laid off as abscissa. The ordinate is the ratio of the column volume to the volume of plug flow apparatus (column of a rather small diameter) providing the same recovery. To estimate the necessary height of the collection zone Hc, the intersection of R(t) = R_0 line (R_0 is the specified recovery) with the line corresponding to Pe value in a commercial column should be found. ~~T~~

~~The plot cannot be used to estimate the height of the collection zone as in the formula for the Peclet criterion Pe=$(U_p + U_f)$H/D the value of H is unknown.~~

4.2.2 Calculation of total recovery.

The next stage of the scaling is the calculation of total recovery in the column R, taking into account material recirculation from the cleaning to the collection zone. Dobby and Finch proposed the two-zone model to estimate the total recovery in collection and froth zones [15,21]

This is described by the formula:

$$R = \frac{R_c R_f}{1 - R_c + R_c R_f},$$

where R_c, R_f are the recoveries in the collection and froth (cleaning) zones, respectievly.
The recovery in the collection zone was estimated from Levenspiel equation. The actual values of the Rf estimated from pilot column tests ranges between 40 and 80% of total recovery [30].

The same authors concluded that collection zone recovery at industrial scale is less (down to 20-50%) [31].

Yianatos et al. proposed a model to estimate froth recovery depnding on superficial gas rate Jg, superficial water rate Jw, and froth depth Hf [32] :

$$R_f = 95\exp[-1.44\cdot 10^{-2}\frac{(H_f(1+3J_w)}{J_g^3}]$$

It provides good correlation between estimated and experimental results. Significant effect of wash water rate upon froth recovery has been demonstrated when Jw increased from 0 to 0.1 cm/s. Froth recovery has been varying in a wider range (from 20% to 70%) comparing to Dobby and Finch papers while overall column recoveries were 40 to 88% at the second copper cleaner circuit of the Colon concentrator at El Teniente (Codelco, Chile).

4.2.3 Calculation of the dispersion coefficients

Several models have been developed to describe Residence Time Distribution (RTD) and dispersion coefficeint D in columns. All of them are based on axial dispersion model and are similar to the equation derived by Laplante et al. 1988 linking *D* to the geomtery of the industrial column (d_c) and air flow reate. One of such approximations can be derived from Kolmogorov's equation

$$\mathrm{D} = 0.35\ \mathrm{d_c}^{4/3}\cdot(\mathrm{g}\cdot\mathrm{J_g})^{1/3}$$

Mixing is more intensive in columns of larger diameter due to irregularity of velocity profile as well as turbulence energy adsorption by the column walls.
Vessel dispersion number can be calculated using the disperson coefficient as

$$N_d = \frac{D}{U_i}\cdot\frac{1}{H_c}\text{,}$$ where U_i =interstitial velocity

Relative phase velocity (interstitial velocity) can be derived from the expression linking superficial feed velocity and gas holdup in the column $\mathrm{U_i} = \frac{J_l}{1-\varepsilon_g}$.

There are many approximation formulas for N_d depending on column parameters. Experiments confirm adequacy of the Kolmogorov's approach [33, 34].

Dobby and Finch propose the following equation for dispersion coefficient and vessel dispersion number [15, 20]

$$D = 0.063 d_c(\frac{J_g}{0.016})^{0.3}$$

$$N_d = \frac{D}{J_p/(1-\varepsilon_g)+U_{sp}}\cdot\frac{1}{H_c}$$

4.2.4 Estimation of flotation rate and slurry residence time

Particle and liquid retention time is estimated according to the following:

Flotation rate can be evaluated by kinetic tests in pilot column to deterimne recovery vs. slurry retention time taking into account wash water rate (or tailings superficial velocity, cm s^{-1}) [15]. Retention time can be changed by varying feed flowrate or collection zone height.

But the reproducibility of the results using this technique is low, therefore, the scale up recommendations are not sufficeintly accurate (see O'Connor et al., 1995). Also, slurry/froth transfer and particle/bubble detachment cannot be ignored in the industrial flotation. Changing the feed flowrate effects all process intensities/rates. If flotation rate cannot be found from pilot or lab-scale column results, it can be estimated using the following aproximations:

$$K = 1.5 J_g E_k / d_b \text{ and } d_b = C J_g^{0.25}$$

where d_b is the mean bubble size estimated by the drift flux analyses [35].

Estimate of axial dispersion model applicability using Dobby and Finch technique is given by Alfrod, et al. [36] and Tuteja, et al [37]. As the result, the new formula for flotation rate has been recommended:

$$K_i = \frac{C_i (J_p - b A_c J_l^{0.75} / Q_c)^{0.75}}{\mu_p}$$

where C_i= mineral-specific parameter, b = constant, Q_c = feed solids flow rate, μ = slurry viscosity. The major conclusion of these papers is to consider one collection zone and not spatially-separated collection zone and froth layer as proposed by Falutsu and Dobby [31].

The technique developed by G. Dobby and J. Finch has the following drawbacks. The effect of hydrodynanic parameters (slurry and air flow rates, type of aerator, etc.) upon the elementary flotation process and stability of flotation aggregate is not estimated, whereas it is one of the main reasons which accounts for difference in commercial process results compared to laboratory test data. As was already demonstrated, the diagram proposed by Levenspiel [38] can not be used to calculate the column height necessary to achieve the specified recovery. The technique does not include calculation of the rise velocity of flotation aggregate. It is known that in countercurrent operation loaded small bubbles are entrained to tailings which results in the reduction of recovery. Froth zone recovery R_f values for the recovered and suppressed components are not assessed from experimental results in the considered work.

4.2.5 Scale-up procedure based on particle/buble attachment/detachment intensities

Scale-up procedure based on separation mass transfer for free and attached particles has been developed and validated. Instead of a single flotation rate, it includes intensity of attachment and detachment processes [27, 29, 30, 40, 63]

$$\frac{dC_p}{dt} = -\mu C_p + \nu C_b - \text{div}(U_p \,.\, C_p) + \text{div}(D_p \,.\, \text{grad}\, C_p)$$

$$\frac{dC_b}{dt} = \mu C_p - \nu C_b - \text{div}(U_b \,.\, C_b) + \text{div}(D_b \,.\, \text{grad}\, C_b)$$

where C_p, C_b are volumetric concentrations of particles in slurry and on bubble surface,
μ, ν are attachment and detachment intensities,
U_p, U_b are the absolute velocities of particles and bubbles, respectively.
Expressions μC_p and νC_b represent transfer of particles from slurry onto bubbles and reverse.
The mass transfer is affected by the column height, velocities U_p and U_b also depend on it.

$$C_p \frac{dU_p}{dx} \neq 0 \; ; \; C_b \frac{dU_b}{dx} \neq 0$$

Raise of hydrostatic pressure with the depth in column as well as bubble coalescence effect air holdup and bubble rise velocity within a column, this has been experimentally confirmed by Gomez et al [41].

Transfer of particles from the slurry onto gas phase determines change in particle velocities within the machine height. Dispersion coefficients for bubbles and particles are also different in various parts of the column.

Therefore, under steady-state conditions, the equations can be represented as

$$0 = -\mu C_p + \nu C_b - U_p \frac{dC_p}{dx} - \frac{dU_p}{dx} \cdot C_p + D_p \frac{d^2 C_p}{dx^2} + \frac{dD_p}{dx} \cdot \frac{dC_p}{dx} + Q/Ac$$

$$0 = \mu C_p - \nu C_b + U_b \frac{dC_b}{dx} - \frac{dU_b}{dx} \cdot C_p + D_b \frac{d^2 C_b}{dx^2} + \frac{dD_b}{dx} \cdot \frac{dC_b}{dx}$$

Expression Q/Ac is attributed to the return of certain flow of particles Q from froth back to the collection zone over column cross-section Ac.

Diagram of particle transfers between different column zones is shown on Figure 4.

Assumptions are that the column has incoming streams of gas, feed slurry and wash water. Particles are discharged into the concentrate with the gas phase and with the slurry and into the tailings only with the slurry. If column is subdivided into N zones with the increment of h (equal to a height of the volume element with ideal mixing within), then the collection zone incorporates zones from 2 to N – 1. In these zones all transfers between slurry and bubbles are allowed. The transfers define the separation process.

Zone 1 is the interface between slurry and froth. Particles are transferred from slurry into concentrate due to the following:
- Displacement of loaded bubbles towards the concentrate;
- Transfer of particles with the liquid and bubbles by dispersion transfer;
- Recycle of particles form the froth as a homogenous phase.

Zone N corresponds to particles leaving the column into tailings stream. Dispersion exchange here exists only with the previous zone N – 1.

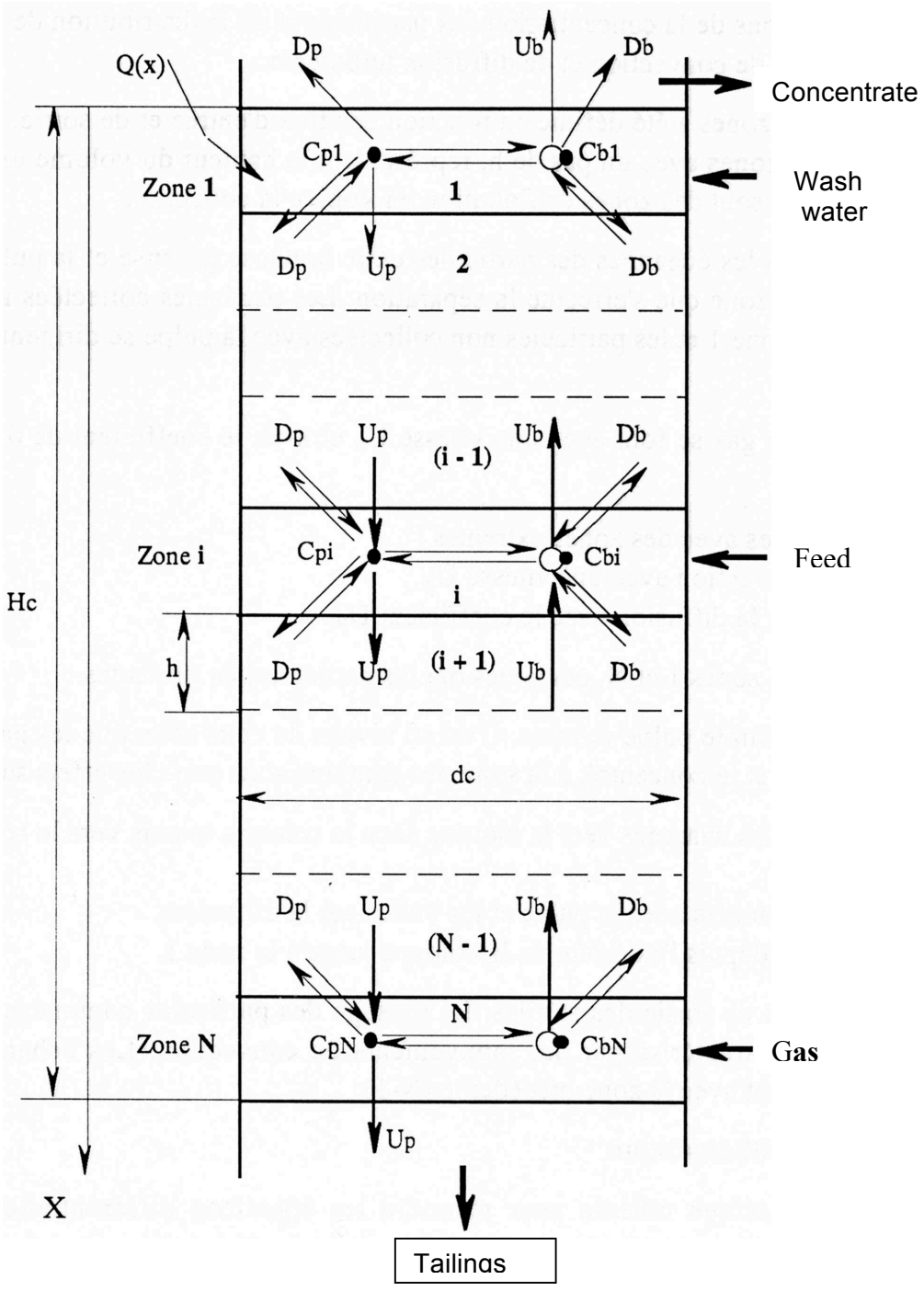

Figure 4. Diagram of transfers in collection zone and connections to external zones. Hc is the height of the collection zone, d_c is the column diameter, Q(x) is the particle flow from froth back to the slurry.

This representation makes possible utilization of finite elements approach to estimate the overall column recovery based on attachment and detachment intensities, particle size distribution in the feed, mean bubble size as well as dispersion coefficient.

Change of gas holdup with the column height affects all major processes in flotation due to shift in the average bubble size. Therefore, equation to estimate D_p based on gas and slurry velocities in addition to the dc/Hc ratio is used [34]:

$$N_d = 1.6\left(\frac{d_c}{H_c}\right)^{0.48} \cdot \frac{J_g^{0.36}}{J_l^{0.47}}$$

or $$N_d = 0{,}56\left[\frac{d_c}{H_c} \cdot \frac{J_g}{J_l} \cdot \left(\frac{J_g}{\varepsilon_g} + \frac{J_l}{1-\varepsilon_g}\right)\right]^{0.41}$$

Another parameter influenced by the average bubble size is the attachment rate m.

It can be estimated based on the formula

$\mu = I_r P_c P_a$.

According to this approach, the adhesion probability P_a is determined by the reagent conditioning and does not change at sale-up. Collision probability P_c is a function of particle and bubble size distributions and can be calculated based on one of the physical or statistical collision models [64].

I_r is the number of events when particle is getting into bubble vicinity (I_r = number of particle–bubble "collisions" per unit time and volume in flotation cells), it depends upon relative particle/bubble velocity and can be determined as

$$I_r = \frac{3}{2} \cdot \frac{U_b + U_p}{d_b} \cdot \frac{\varepsilon_g}{1-\varepsilon_g}$$

Relative particle velocity in the slurry can be calculated by hindered settling equation by Masliyah [24]:

$$U_{pi} = \frac{g d_{pi}^2 \cdot (\rho_p - \rho_l)(1-\varepsilon_s)^n}{18\mu_l(1 + 0.15\,\mathrm{Re}_{ls}^{0.687})}$$

and

$$\mathrm{Re}_{ls} = \frac{d_{pi}^2 \rho_l U_{pi}(1-\varepsilon_s)}{\mu_l}$$

with ε_s = solids hodup in the slurry, μ_l =viscosity of the slurry. Accoring to RICHARDSON and ZAKI [65] parameter *n* above depends on mixing and is equal to 2.7 for Re<1000.

The overall collision intensity is $I_c = I_r P_c$.

Collision probability for coarse particles can be calculated by Langmuir equation

$$P_c = \left(\frac{Stk}{Stk + 0.2}\right)^{0.2} \text{ and } \quad Stk = \frac{1}{9}\frac{U_b d_p \rho_p}{d_b \mu_l}$$

or by Flint and Howart [60]

$$P_c = \frac{G}{1+G} \text{ with } \quad G = \frac{U_p}{U_b}$$

For intermediate bubble Reynolds number in the range of 0.2 < Reb < 100, the equation proposed by Yoon *et al* for the collision probability can be applied [54] *:*

$$P_c = \left(1.5 + \frac{4}{15} Re_b^{0.72}\right) \frac{d_p^2}{d_b^2}$$

where the bubble Reynolds number ~~based on~~ $Re_b = d_b U_b/\mu$ is used. The equation is valid for particles smaller than 100 μm and bubbles smaller than 1 mm with surfaces immobilised due to adsorbed surfactants.

Detachment intensity can be evaluated by experimental results or by iteration method which assumes that ratio between attachment and detachment rates is more important that their absolute values [29]. The model has been verified when attachment and detachment rates as well as particle recycle rate from the froth have been estimated using empirical techniques [39]. Simulation results have been compared with 200 mm dia. pilot column in cassiterite scavenger flotation.

The parameters μ, ν and K_b (drop back probability describing the Q_r) are estimated by a preliminary tests in lab scales [42,43]. Values of parameters (μ, ν and K_b) were taken as the first approximation for modelling. The comparison of the calculated recovery of tin for each class (28, 56 and 100 μm) of particles and the distribution of the losses of cassiterite in the tailings ~~product~~ allows to validate the intensities obtained by the model. The results of the validation are presented in Table 1.

Table 1: Modelling and validation results of cassiterite column flotation in pilot-scale machine (adapted from [39])

Test No.	J_a, cm/s	J_g, cm/s	Average bubble diameter mm	Gas hold-up %	Attachment intensity (10^{-3} s^{-1}) drop-back probability for particle size (μm)			Sn Recovery, %	
					28	56	100	Calculated	Pilot test
1	0.8	1.3	1.2	11.8	5.0 0.75	4.2 0.8	2.8 0.8	59.8	60.0
2	1.1	1.3	1.2	11.8	5 0.75	4.2 0.8	2.8 0.8	56.5	58.8
3	1.8	1.3	1.1	10.9	5.0 0.75	4.2 0.75	2.8 0.8	40.5	43.8
4	3.3	1.3	0.9	12.9	5.0 0.75	4.2 0.75	2.8 0.8	26.4	42.1
5	0.8	2.3	1.4	14.2	5.0 0.7	4.5 0.75	3.3 0.8	70.3	73.3
6	1.1	2.3	1.3	16.5	5.5 0.65	4.5 0.7	3.3 0.75	67.3	68.2
7	1.8	2.3	1.4	14.3	6.5 0.65	5.5 0.67	4.3 0.7	63.7	66.8

8	3.3	2.3	1.2	19.8	6.5 0.6	5.5 0.67	4.3 0.7	45.7	52.4

The model validation procedure is required to compare experimental and calculated recoveries for different superficial gas velocities J_g by regrouping close superficial feed velocities J_l. This approach is justified by the fact that the important variations of J_l induce a variation of the bubble diameter; consequently, the estimate of the bubble-particle collision probability is distorted. The possibility to calculate the size-by-size particle distribution by column height and to compare it with the experimental distributions constitutes the next level of parameter validation.

Thus, the model validation results demonstrate the applicability limits for the axial diffusion model ~~related to the qualitative changes on considered basic phenomena~~.

Further development of this scale-up approach has been done by comparison of calculated and measured particle profile along the column height [40].

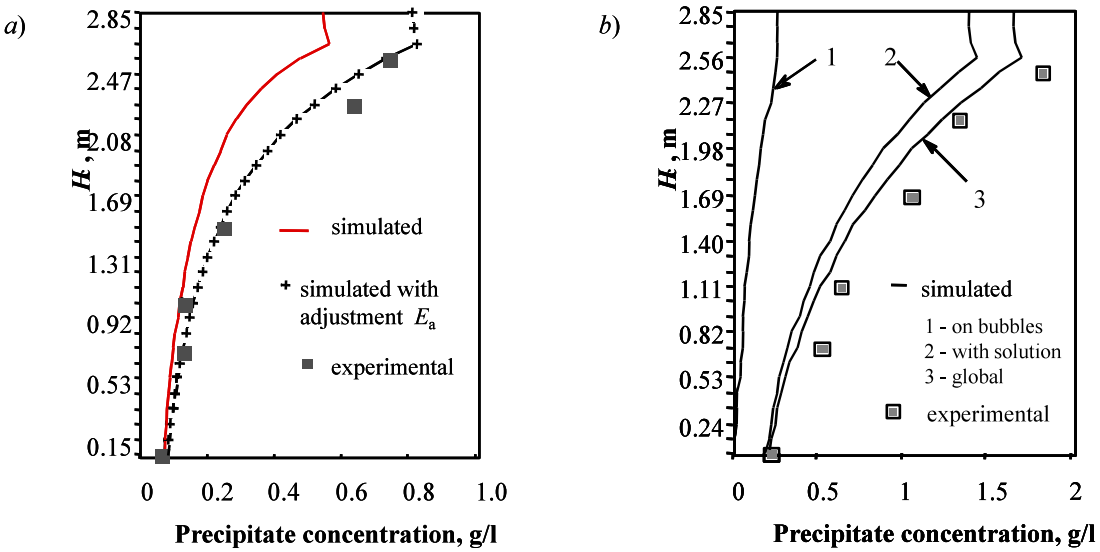

Figure Simulated and experimental concentration of molybdenum precipitate particles as a function of column height Hc:
a) J_l = 0.19 cm/s, b) J_l=0.47 cm/s.
Ea is energy dissipation that effects the ~~particle~~ precipitate particles size and, therefore, the attachment rate μ.

This allows to adjust finite elements calculations based on process intensities (rates) as well as on gas holdup changes and, therefore, dispersion number fluctuations.

4.2.6 Deviation of flotation from the first-order kinetics

To assess bubble load (the fourth stage of scaling procedure), formulas were derived to calculate the mass of solids per unit air volume. Collection rate is assumed to be constant in the period when loading is below 80% of the bubble surface.

The major limitation of flotation kinetic models is considerations for free bubble surface and maximum bubble carrying capacity. Fuerstenau and Sastry [17] used

two-phase separation mass transfer approach including attachment K_1 and detachment K_2 rate coefficients.

$$D_p \frac{d^2 C_p}{dx^2} - U_p \frac{dC_p}{dx} - \hat{E}_1 A_v C_p \left(1 - \frac{C_b}{C_b^*}\right) + K_2 A_v C_b = 0$$

$$D_b \frac{d^2 C_b}{dx^2} - U_b \frac{dC_b}{dx} + \hat{E}_1 A_v C_p \left(1 - \frac{C_b}{C_b^*}\right) - K_2 A_v C_b = 0$$

In these equations, kinetic restrictions are introduced by A_v member which is the interphase liquid/gas surface area and by C_b^* which is maximum particle concentration on bubbles. But the paper does not include the methods to find these parameters. Similar approach has been used by Filippov [39] to estimate the bubble rise velocity reduction by mineral load; it is based on experimentally confirmed flotation kinetics [42,43]. It has been demonstrated that reduction in upward bubble velocity better describes flotation comparing to the approach based on the limits of bubble surface. The rate of bubble velocity reduction has been expressed as

$$K_b = \frac{\rho_l - (C_b - \rho_p)/\varepsilon_g}{\rho_l}$$

The most common technique to estimate bubble load by particles is column carrying capacity calculation developed by Canadian researchers [45-47]. Carrying capacity is expressed as C_a, g/(min cm^2). It can be estimated using the approximation formula .

A tentative model is presented to predict column carrying capacity (C_a) as a function of particle size (d_{80}) and particle density r_p: $C_a = 0.068\ (d_{80} \times r_p)$. Evidence is presented suggesting C_a is independent of column diameter.

$$C_a = \frac{0{,}06 \cdot \psi \cdot \pi \cdot d_p \cdot \rho_s \cdot J_g}{d_b}$$

ψ depends upon bubble loading and size difference as well as probability of detachment in froth.
d_p and d_b are particle and bubble size, respectively,
J_g is superficial air velocity (see below)
ρ_s is the solids density.

Average experimental value of ψ is close to 0.6. It is preferable to use experimental values for the scale-up rather than calculated based on empirical model [48]. Sastri [49] revised the equation proposed by Espinosa-Gomez et. al. [45] for the carrying capacity in flotation columns to obtain better fit to the data. Flotation columns are found to be normally operated at about 60% of their maximum carrying capacities.

The fact that the collection of mineral particles by bubbles greatly depends on the amount of bubble surface available was criticized by Bouchard et al. (2009) They note that the more adequate way to take into account the influence of gas to the flotation process is to use bubble ***surface area flux*** - the amount of bubble surface per unit time and unit of column cross section area instead of the gas hold-up. This becomes obvious when comparing the flotation performance of similar volumes of air

in the form of a swarm of small bubbles (large specific area) or a swarm of fewer larger bubbles (smaller specific area). The expression for bubble surface area flux Sb can be derived from the definition and includes the superficial gas velocity and mean bubble diameter d_b as follows:

$$S_b = 6J_g / d_b$$

Yoon and co-authors used Peclet number and vessel dispersion number N_d to evaluate mixing. Their approach is also based on axial dispersion model [52, 54, 55, 57] and lead to development of a static simulator based on hydrodynamic principles, aiming at predicting the recovery of a column flotation operation. Peclet number estimate included effect of the column geometry (H_c, d_c) and flow rates (Jg, Jl) as well as gas holdup ε_g [56].

$$Pe = 0.6\left(\frac{H_c}{d_c}\right)^{0.63} \cdot \left[\frac{J_l}{J_g(1-\varepsilon_g)}\right]^{0.5}$$

In their initial papers, these researchers proposed using the following formula for flotation rate depending on bubble diameter and gas holdup to calculate collection zone recovery

$$K = \frac{3}{2} \cdot \frac{P_c}{d_b} \cdot J_g$$

Later, maximum carrying capacity has been calculated as a product of free bubble surface and bubble load presented as

$$\tilde{N}_a = 4d_p \cdot \rho_p J_g \cdot \beta / d_b$$

where ρ_p is particle density and β depends upon packing of particle on bubble surface.

4.2.6 Conclusions

4.2.6.1 Conclusions on the considered models

Application and evaluation of flotation kinetic models based on axial dispersion approach allowed to indicate the limits of their applicability.

1. Major drawback of all models is lack of froth analysis. Description of interaction between collection zone and froth layer is based on experimantal observations and empirical relationships.
2. Models do not take into consideration radial mixing in columns
3. Analytical solution of diffusion equation assumes first-order kineteics. Models using two-phase separation mass transfer equations (particle transfer by slurry and by bubbles) require identification of both attachment and detachment rates.
4. Majority of models do not consider the composition of flotation feed.
5. It is extremely difficult to include products grade into models to compare simulation outcome to metallurgical results of column flotation.

4.2.6.2 Conclusions on the scale-up procedure

Scale-up methodology includes pilot-scale testing and is comprised of the following traditional stages:

1. Fesability studies to define the limits ot the major operating parameters (gas and slurry flow rates)

2. Kinetic tests to determine flotation rate for different mineral components based on dependency of recovery from retention time in the column (attained by changing J_l or collection zone height)
3. Determine bubble carrying capacity using one of the empirical formulas
4. Study of mixing in the column (dispersion number Nd, dispersion coefficient D, or Peclet number Pe) using empirical or analytical dependencies
5. Find particle and liquid retention time in the machine based on feed flow rate Jl and particle settling velocities

Evaluate mean bubble size using drift flux analysis method

6. Parameter identification and calculation of the recovery of components in the collection zone by Levenspiel equation
7. Estimate overall column recovery including froth recovery
8. Comparison of model and epxerimental results and defining the column diamter required to provide the given Jl. Iterative approach using different superficial feed velocities may be needed.
9. Number of industrial columns is determined.

The simplified approach proposed by Yoon can also be utilized.

Equation for carrying capacity depending on column diameter is used:

$$C_a = \frac{4M_f Y}{\pi N d_c^2}$$

where Ca is determined from the tests, Mf is the capacity by solids, *Y* is the flow of the concentrate and *N* is the number of machines.

Column diameter is determined based on the volumetric feed flow rate and the solids content in the feed *s*:

$$d_c = \sqrt{\left[\frac{4Y}{\pi C \max}\left(\frac{1}{\rho_p} + \frac{1-s}{s}\right)^{-1} \cdot \frac{Q_p}{N}\right]}$$

Column height is then calculated by combining retention time, superficial feed velocity J_l and superficial wash water velocity J_b

$$H_c = \tau_p \left[\frac{J_l + f J_b}{1-\varepsilon_g} + U_p\right]$$

Levenspiel equation is used to include mixing characteristics.

The two approaches above (with some modifications) are used in the industry for column flotation machines scale up.

References

1. Yianatos J.B., Bergh L.G., Aguilera J. Flotation scale up: use of separability curves, Min. Eng., 16, 347-352 (2003).

2. Rubinstein J. B. Column flotation: Processes, Design and Practives, 204-221 (1995).

3. Nguyen P.T., Nguyen A.V. Validation of the generalised Sutherland equation for bubble–particle encounter efficiency in flotation: Effect of particle density, Minerals Engineering 22, 176–181 (2009)

4. Derjaguin, B.V. , Dukhin, S.S. , Rulyov, N.N. in: E. Matejevic, R.J. Good (Eds.), Surface and Colloid Science, Vol. 13, Wiley–Interscience, New York, 1984, Chap. 2,

5. Pyke B., Fornasiero D., Ralston J. Bubble particle heterocoagulation under turbulent conditions, Journal of Colloid and Interface Science 265, 141–151 (2003).

6. Samygin V.D., Margulis L.G., Burstein M. Calculation of flotation rate constant according to the subprocess structure with accounting the space heterogeneity, Izv. Vuzov. Tzvet. Metall. 2, 12-18 (1985).

7. Ralston J., et al. Reducing uncertainty in mineral flotation—flotation rate constant prediction for particles in an operating plant ore, Int. J. Miner. Process. 84 , 89–98 (2007)

8. Koh P.T.L., Schwarz M.P., CFD modelling of bubble–particle attachments in flotation cells, *Minerals Engineering* 19, 619–626 (2006).

9. Koh P.T.L., Schwarz M. P., Modelling attachment rates of multi-sized bubbles with particles in a flotation cell, Minerals Engineering, 21, 989-993(2008).

10. Gorain B. K., Harris M. C., Franzidis J.-P., Manlapig E. V. The effect of froth residence time on the kinetics of flotation, Minerals Eng. 11, 627-638 (1998).

11. Schubert H. On the optimization of hydrodynamics in fine particle flotation, Minerals Eng., 21,930-936 (2008)

12. Newell R., Grano S. Hydrodynamics and scale up in Rushton turbine flotation cells:Part 2. Flotation scale-up for laboratory and pilot cells, Int. J. Miner. Process. 81, 65–78 (2006)

13. Yianatos J.B., Diaz F., Rodriguez J., Industrial flotation process modeling: RTD measurement by radioactive tracer technique. In: 15th IFAC World Congress, Barcelona, Spain, 21–26 July 2002.

14. Cilek E.C. The effect of hydrodynamic conditions on true flotation and entrainment in flotation of a complex sulphide ore, Int. J. Miner. Process. 90, 35–44 (2009).

15. Dobby G.S., Finch J.A. Flotation column scale-up and modeling. CIM Bulletin, 79 (889), 89-96 (1986).

16. Rubinstein J.B., Melik-Gaikazyon V.I., Matveenko N.V., Leonov S.B. Foam

separation and comumn flotation. Moscow: Nedra Publishers, p. 93-290 (1986).

17. Sastry K.V.S. Processing of mineral fine by column flotation. Final report of california Institute of Mining and Mineral Processing, University of California. Sponsored projects CA-80-MPS(4) and Grant n°G5105014. DOI –OSM-MB-7910. (1981).

18. Finch J.A. and Dobby G.S. Column Flotation. Pergamon Press. (1990)

19. YIANATOS J.B. Flottation en Colonne. Etat actuel de la technologie. Mines et Carrières, Les Techniques, 213, 31-40 (1990).

20. DOBBY G.S. and FINCH J.A. Mixing Characteristic of Industrial Flotation Columns. Chem. Eng. Sci., 40(7), 1061-1068 (1985)

21. DOBBY G.S., FINCH J.A. Particle Collection in Columns-gas rate and bubble size effects. Can. Metal. Quart, 25(1), 89-96 (1986)

22. DOBBY G.S. and FINCH J.A. Estimation of Bubble Diameter in Flotation Columns from Drift Flux Analyses. Can. Met. Quarterly, 27 (2), 85-90 (1988)

23. Yianatos J.B., Finch J.A., Laplante A.R. Apparent Hindered settling in a gas-liquid-solid countercurrent column. Int J of Mineral processing, 18 (3/4), 155-165 (1986)

24. Masliyah J.H. Hindered settling in a multi-species particle system. Chem. Eng. Sci., 34,1166-1168 (1979)

25. Levenspiel, O . Chemical Reaction Engineering. Wiley M.Y., Chapter 9, (1972).

26. Sastry K.U.S. and Furstenau D.V. Theoretical analysis of a countercurrent flotation column. Trans. Soc. Min. Eng. AIME, 247 (1) 46-52 (1970).

27. Samyguin V.D., Filippov L.O. and Burstein M. Yu. Dispersion Axial Models of Froth Flotation. Izvestiya Vuzov. Tsvetnaya Metallurgiya, 3, 3-8 (1985).

28. Ityokumbul M. T. A mass transfer approach to flotation column design Chemical Engineering Science, 47(13-14), 3605-3612 (1992).

29. Shekhirev, D.V. Filippov, L.O. Samyguin V.D. Mathematical Modelling the Process of Separation of the Raw Materials in the Column Flotation Machine. *Proceedings* XVIII International Mineral Processing Congress**,** Sydney Australia, 23-28 mai 1993, Aus IMM, vol. 5, pp. 1357-1362 (1993).

30. FALUTSU M. and DOBBY G.S. Direct Measurment of Froth Dropback and Collection Zone Recovery in a Laboratory Column. Minerals. Engineering, 2(3), 377-386 (1989)

31. Falutsu, M., Dobby, G.S., "Froth Performance in Commercial-Sized Flotation columns". Minerals Engineering, 5 (10-12) 1207-1223 (1992).

32. Yianatos, J.B., L.G.Berg and G.A.Cortés Froth zone modelling of an industrial column . Min. Eng. 11 (5), 423-435 (1998).

33. Baird M.H.I., Rice R.G. Axial dispersion in large unbaffled columns. The Chemical Engineering Journal, 9,171-174 (1975).

34. MANQUI Xu and FINCH J.A. (1991) Estimating Vessel Dispersion Number in Flotation Columns. Column' 91, Sudbury, Canada, CIM (Agar G.E., Huls B.J., Hyma D.B., and Herbst J.A. Editors), 2, p. 437-454.

35. YIANATOS J.B., FINCH J.A., DOBBY G.S. and MANQUI XV. Bubble Size Estimation in a Bubble Swarm, Journal of Col. and Interf. Sci., 126 (1), 37-44 (1988)

36. ALFROD R.A., BIJOK A., BAGULEY and ARTONE Column Flotation Design at Peak Gold. Proceedings Column'91 (G.E. Agar, B.J. Huls and D.B. Hyma Eds), 1991, Sudbury, Ontario, Canada, p. 123-136 (1991).

37. Tuteja, R.K., D.J. Spottiswood and V.N. Misra . Mathematical models of the column flotation process: a review . Minerals Engineering, 7 (12), 1459-1472 (1994).

38. Rubinstein J.B., Melik-Gaikazyon V.I., Matveenko N.V., Leonov S.B. Foam separation and column flotation. Moscow: Nedra Publishers, p. 93-290

39. Filippov L.O. Column flotation of low cassiterite contained slime's : Modelling and Scale-up using pilot plant data. *Developments in Mineral Processing's"*, Elsevier, vol. 3, pp. A3-8 – A3-15 (2000).

40. Filippov L.O. and Filippova I.V. Regularities in precipitate flotation in a column. *Proceedings* of the XXII International Mineral Processing Congress, (L. Lorenzen and D.J. Bradshaw Eds.), Cape Town, South Africa, September 28 - October 3, SAIMM, 2003, vol. 2, pp. 1072-1083.

41. Gomez, C.O. Uribe-Salas A., Finch J.A. and Huls B.J., Axial gas holdup profiles in the collection zone of flotation columns, Miner. Metall. Process. 12 (1), 16–23 (1995)

42. L.O. Filippov, V.D. Samyguin, D.V. Krapivnyi, D.V. Shekirev. Determination of hydrophobic and froths form properties of non ionic reagents from froth flotation kinetics. *(rus) Obogatshenie rud* 41-48, (1990).

42. L.O.Filippov and R.Houot. Synergistic effects of a non ionic reagent with heteropolar collectors on the non sulphide ores flotation *Proceedings* of the XX International Mineral Processing Congress, (H., Hoberg and H. von Blottnitz Eds.), Aachen, Germany, September 21-26, 1997, vol. 3, pp. 427-436.(1997)

43. Samyguin, V.V.,Tchertilin, B.D., Nebera, V.P. Kolloidnyi Zh., 39, (6), 1101-1107. (1977).

44. Samygyin V.D, L.O.Filippov, B.S.Tchertilin. Kinetic of equal rate particles flotation under frothless conditions in respect of rising bubble velocity's *Izvestiya Vuzov. Tsvetnaya Metallurgiya*, 5, 4-9 (1982)

45. ESPINOSA-GOMEZ R., FINCH J.A., YIANATOS J.B. and DOBBY G.S. Column Carring Capacity : Particle Size and Density effect. Minerals Engineering, 1(1), p. 77-79, (1988)

46. ESPINOSA-GOMEZ R., JOHNSON N.W., FINCH J.A. (1989) Evaluation of Flotation Column Scale-Up at Mount Isa Mines Limited. Minerals Engineering, 2(3), p. 369-375.

47. Espinosa-Gomez, R and Johnson, N W, 1991. Technical Experiences with Conventional Columns at Mount Isa Mines Ltd. Proceedings Column'91 (G.E. Agar, B.J. Huls and D.B. Hyma Eds), 1991, Sudbury, Ontario, Canada, Vol. 2, pp511-523.

48. Del VILLAR R., GOMEZ C., FINCH J.A. et ESPINOSA R. Etudes de faisabilité et Conception Préliminaire des Colonnes de Flottation. Mines et Carrières, Les Techniques, 2/3, p. 92-96. (1990)

49. Sastri S. R. S. Carrying capacity in flotation columns, Minerals Engineering, 9 (4) 465-468 (1996).

50. Bouchard, J., Desbiens, A., del Villar,R., Nunez E. Column flotation simulation and control: An overview Minerals Engineering, 22(6), 519-529 (2009).
51. J. Bouchard, A. Desbiens, R. del Villar Recent advances in bias and froth depth control in flotation columns. Minerals Engineering, (18), (7), 709-720 (2005).

52. ADEL G.T., M.J. MANKOSA, M.J. LUTTRELL, G.M. YOON, R.H.,
Full-Scale Testing of Microbubble Column Flotation. Proceedings Column'91 (G.E. Agar, B.J. Huls and D.B. Hyma Eds), 1991, Sudbury, Ontario, Canada, p. 263-274. (1991)

53. Laplante, AR, Yianatos, J. and Finch, JA, 1988. On the mixing haracteristics of the collection zone in flotation columns. Proc. of an Int. Column Flotation Symp. Phoenix, Arizona, Jan., Chap. 9, pp. 69 – 79.

54. Luttrell, G., Mankosa, M., Yoon, R.-H., 1993. Design and scale-up criteria for column flotation. In: XVIII International mineral Processing Congress, Sydney, pp. 785–791.

55. Luttrell, G., Yoon, R., A flotation column simulator based on hydrodynamic principles. International Journal of Mineral Processing 33, 355–368 (1991).

56. Mankosa, M.J., Luttrell, G.H., Adel, G.T., and Yoon, R.-H. "A Study of Axial Mixing in Column Flotation," International Journal of Mineral Processing, vol. 35, pp. 51-64 (1992).

57. Yoon, R.-H., Luttrell, G.H., Adel, G.T., and Mankosa, G.T., The Application of Microcel Column Flotation to Fine Coal Cleaning, Coal Preparation, 10, 177-188 (1992).

58. YIANATOS J.B., LAPLANTE A.R. and FINCH J.A. Estimation of Local Holdup in the Bubbling and Froth Zones of a Gaz-Liquid Column. Chem. Eng.Sci., 40(10), p. 1965-1968. (1985)

59. Finch, J. A., Dobby, G.S. Column flotation: A selected review. Part I. International Journal of Mineral Processing, 33, (1-4) 343-354 (1991).

60. Flint, R.L. and Howarth, W.J., The Collision Efficiency of Small Particles with Spherical Air Bubbles. Chemical Engineering Science, 26, 1155-1168 (1971)
61. O'Connor C.T. , Mills P.J.T., Cillier J.J. Prediction of large scale column flotation cell performance using pilot plant data. Chem. Eng. J., 59, 1-6

62. Mills P.J.T., C.T. O'Connor .The use of the axial dispersion model to describe mixing in a flotation column. Minerals Engineering, 5 (8), 939-944 (1992).

63. Sastry, K.V., Lofftus, D.D., Mathematical modeling and computer simulation of column flotation. In: Sastry, K.V.S. (Ed.), Column Flotation'88. SME, Littleton, CO, USA, pp. 57–68. (1988)

64. Koh P. T. L., Schwarz M. P. CFD modelling of bubble–particle collision rates and efficiencies in a flotation cell. Minerals Engineering, 16 (11) 1055-1059 (2003).